energies

MDPI

Article

Experimental and Simulation Studies of Energized Fracturing Fluid Efficiency in Tight Gas Formations

Klaudia Wilk

Department of Production Stimulation, Oil and Gas Institute—National Research Institute; Lubicz 25A Str., 31-503 Krakow, Poland; klaudia.wilk@inig.pl

Received: 19 September 2019; Accepted: 19 November 2019; Published: 23 November 2019

Abstract: The use of water-based fracturing fluids during fracturing treatment can be a problem in water-sensitive formations due to the permeability damage hazard caused by clay minerals swelling. The article includes laboratory tests, analyses and simulations for nitrogen foamed fracturing fluids. The rheology and filtration coefficients of foamed fracturing fluids were examined and compared to the properties of conventional water-based fracturing fluid. Laboratory results provided the input for numerical simulation of the fractures geometry for water-based fracturing fluids and 50% N_2 foamed fluids, with addition of natural, fast hydrating guar gum. The results show that the foamed fluids were able to create shorter and thinner fractures compared to the fractures induced by the non-foamed fluid. The simulation proved that the concentration of proppant in the fracture and its conductivity are similar or slightly higher when using the foamed fluid. The foamed fluids, when injected to the reservoir, provide additional energy that allows for more effective flowback, and maintain the proper fracture geometry and proppant placing. The results of laboratory work in combination with the 3D simulation showed that the foamed fluids have suitable viscosity which allows opening the fracture, and transport the proppant into the fracture, providing successful fracturing operation. The analysis of laboratory data and the performed computer simulations indicated that fracturing fluids foamed by nitrogen are a good alternative to non-foamed fluids. The N_2-foamed fluids exhibit good rheological parameters and proppant-carrying capacity. Simulated fracture of water-based fracturing fluid is slightly longer and higher compared to foamed fluid. At the same time, when using a fluid with a gas additive, the water content in fracturing fluid is reduced which means the minimization of the negative results of the clay minerals swelling.

Keywords: hydraulic fracturing; energized frac fluids; reservoir stimulation; tight gas; fracturing fluids rheology

1. Introduction

Considering the continuing depletion of energy resources in the world [1,2], the extraction of natural gas has become a priority and it is believed to be a more ecological solution than the extraction of high-emission solid fossils. Hydraulic fracturing is the most efficient method for stimulating hydrocarbon deposits [3] and has been used for many years to produce gas from deep and poorly permeable geological formations. Multistage fracturing of horizontal wells significantly improves the production performance of low and ultralow permeability gas reservoirs. One of the fundamental components of hydraulic fracturing treatment is fracturing fluids that ensure transport of proppant into the fractures. Fracturing fluids based on polymers such as guar and guar derivatives have been widely used for fracturing treatments, but polymer based fluids could cause serious formation damages and may cause numerous environmental problems [4–6], which is why alternative solutions are tested, among which the use of foamed fluid is a relatively new but effective technique [7]. Foamed fluid is generated by mixing the gaseous phase with the liquid phase, in the presence of a proper surface-active

agent. The primary parameter of such fluid, so-called foam quality, depends on the percentage of gas in the fracturing fluid [8,9]. The quality of fluid is determined by the following formula (Equation (1)):

$$Q = (V_g) / (V_g + V_l) \cdot 100 \quad (1)$$

where Q = foam quality, V_g = gas volume, V_l = volume of liquid in the foam.

Foam and energized fluids are composed of one compressible component such as carbon dioxide or nitrogen that are considered to overcome the formation damage and clean-up efficiency of conventional fracturing fluids especially in tight unconventional formations. The properties of foam injected into a deposit, including its rheology and viscosity, are important for the success of the fracturing process. The viscosity of foamed fluid should be high enough at the beginning to provide good proppant transport, and low enough at the end of fracturing treatment to get good clean up of fracture and formation. Better transport properties for the proppant, lower consumption of water and chemicals, a faster and easier flowback and potentially a lower environmental impact—these are the advantages of fracturing with foamed fluids [10]. On the other hand, there is still lack of knowledge and an insufficient amount of experimental research related to the use of foams. Furthermore, high costs and potential harm to the environment caused by surface-active agents constitute limitations in the use of this technology, while technical requirements for foam generation process (equipment, separate storage facilities of liquid, gas, surfactants, and proppants) are one of the main drawbacks of the foam-based fluid fracturing [11].

The search for new technologies stimulating extraction from unconventional deposits is related to the issue of reducing water consumption [12–14], as well as the aspect of sensibility of clay minerals to contact with water [15] and extending the productive lifetime of each well [14]. The elimination or reduction of the water amount for the fracturing fluid can be a significant advantage in the dissemination of alternative technologies.

The process of hydraulic fracturing of unconventional deposits, especially those which are characterized by low reservoir pressures, and sensitive to contact with water, is performed very frequently with the use of foams or energized fluids [16,17]. Compressed gas which is present in the foam (e.g., nitrogen), expand during the clean-up of fracturing fluid, facilitating the removal of fluid from the fracture. Foams accelerate the flowback from a propped fracture and this is why they are suitable for use in deposits with low reservoir pressures [18]. In the case of water-based fluids, their foaming causes a considerable decrease in the amount of liquid which is in contact with the reservoir formation [19], since such a fluid can contain up to 95% by volume of gas. Harris at al. (1996) conducted research for 95% nitrogen content foam, trying to use different combinations of additives to produced stable foams at lower quality [20]. The selection of the foam quality, liquid phase and gas types depends on economic aspects and reservoir conditions (rock permeability and porosity, water availability, reservoir temperature, pressure, clay content, etc.). This is why foams are also recommended in the case of deposits particularly sensitive to contact with water due to water absorption into the clay minerals structure. Their use allows a significant reduction of water necessary for fracturing operations [21,22]. Due to this, there is a considerable decrease in the costs of its purchase, transport and preparation, including clean up, and the costs of chemical additives, as well as the costs of storage and subsequent post-treatment fluids purification.

Currently, on the market there are several available commercial simulators used by reservoir engineers for designing and analyzing hydraulic fracturing operations [23–27]. Based on the collected reservoir data as well as fracturing fluids and proppant data, precise and advanced design of hydraulic fracturing operations is possible [28], including the use of foamed fluids. According to McAndrew et al. (2014), fracture length, height and conductivity are mostly dependent on the fracturing fluid type. Authors simulated the fracture conductivity using slick water, 75% quality CO_2 foams, and 75% quality N_2 foams. Although slick water provides a longer fracture compared to 70% quality N_2 foams, it does not deliver proppant in the whole fracture length and height. It has been also shown that for fractures created with foam, the fracture length is smaller, but the proppants are delivered to a

larger area of the fracture. CO_2 and N_2 foams provide very similar proppant placement [29]. Foam as fracturing fluid performs better in terms of proppant transportation with higher corresponding fracture conductivity than water based fracturing fluids [30]. Fei Y. et al. showed that the foam quality could contribute to a higher fracture pressure. This is because higher viscosity of foam improved leakoff control, with greater proppant carrying capacity comparing with slickwater to increase fracture conductivity. For 3D hydraulic fracture, simulation in a vertical well was developed and validated with postfrac production data and sensitivity analysis was performed using a selection of different fracturing fluid treatments. It was found that the use of foam results in a more rapid clean-up of the fracture itself and inside the wellbore, which is expected to provide higher productivity. Gu et al. studied foam fracturing using polymer free foam considering ultra-lightweight proppants [31,32]. They also developed empirical correlations through the modification of the power law model, which were then applied in a fracturing and reservoir model using a commercial simulator CMG IMEX. They used ultra-lightweight proppants to predict the formation productivity with foams. Foam-based hydraulic fracturing fluid utilized less water compared to that of slickwater fluid.

For this paper a commercial fracture simulator (Fracpro) was used to simulate fluid design and fracture properties, and it allows users to import a type of fracture growth behavior that may be unique to a certain formation. The 3D shear-decoupled model (version 10.3.) predicts longer and more confined hydraulic fractures caused by the introduction of a composite layering effect (CLE). This model is used to simulate fracture growth behavior for this research because layered tight gas sands have been shown to exhibit this behavior [33].

2. Materials and Methods

2.1. Sample Preparation

Foamed fracturing fluid was created based on tap water with the addition of N_2. At first, the following components were added to water with a temperature of 23 °C: an anionic foaming agent P-1 (4 mL/L), a microemulsion M-1 (2mL/L), a clay-swelling inhibitor C-1 (2mL/L), a scale inhibitor S-1 (1mL/L), followed by polymer W (natural, fast hydrating guar gum for oil field applications) in an amount of 3.6 g/L. Additives to fracturing fluids were selected based on previous works, which allowed the assessment of the best additives for the foamed fluids [34,35].

The samples of rock material representing Rotliegend sandstone from the Poznan Trough, Poland (a tight-type formation) were used for tests. The analyzed cores represent aeolian sandstones originating from a deposit situated in the top part of upper Rotliegend sediments belonging to a Permian–Mesozoic structural unit. Numerous natural fractures occur within Rotliegend rocks. The medium which saturates the sandstones is a nitrogen-rich natural gas with a methane content of approximately 75–80 vol.%, lacking gasoline, with a high carbon dioxide content and with no hydrogen sulphide.

The preparation of samples involved the cutting of cylindrical core plugs, 3.8 cm in diameter and approximately 2.5 cm high. Core plugs were dried at a temperature of 105 °C for 24 hours. After drying and cooling the cores, the gas permeability coefficient was determined for each of them using a DGP-100 apparatus, (EPS, UK), along with the effective porosity coefficient measured by means of an HGP-100 (EPS, UK) helium porosimeter. Measurements of the fracturing fluids rheological parameters were made using a pipe rheometer with a foam generator, and measurements of leakoff coefficients were made by means of combining a pipe rheometer with a leak-off chamber and an HPLC pump (Sykam, GE).

2.2. Rheology

A fracturing fluid (prepared according to the description in Section 2.1) was introduced into the pipes of rheometer designed specifically to measure the rheological properties of foamed fluids under extended pressure and temperature conditions, and the fluid was stirred at a rate of 300 s^{-1} in the measurement system [7,36]. At the same time, the temperature and pressure were stabilized

(6.89 MPa, T = 23 °C or T = 60 °C). Subsequently, in the case of measuring foamed fluids, N_2 was slowly injected into the measurement system, continuously stirring the fluid in the system with a shear rate of 350 s^{-1}. Simultaneously, the fluid followed by partially foamed fluid was collected from the system, increasing the gas content in the foam. This process was performed until reaching 50% foam quality, which was controlled by a densimeter. Once the foam quality stabilized, measurements of the rheological properties were started in accordance with the prepared test plan. The test lasts 27 minutes, at a pressure of 1000 psi, maintaining a shear rate of 100 s^{-1}. To measure the rheological properties during measurement loops (at minute 9, 18, and 27), the shear rates were assumed as follows: 40, 100, 200, 300, 200, 100, 40 s^{-1}. During a measurement loop, the shear rate was kept at each of the aforementioned levels for 30 s to obtain a stable result. Between measurements, the foam was stirred at a rate of 100 s^{-1} for approximately 5 min.

2.3. Filtration Measurements

Filtration tests were performed under static conditions according to a modified measurement procedure originating from quality standard API RP39 [7,37], involving the tests of fracturing fluids and examinations of the leakoff coefficient. The core intended for tests was seated in a measurement chamber using high-temperature silicone. Then, the remaining elements of the measurement chamber were assembled and it was left for approximately 24 h. Next, the chamber was thermostatted to a temperature of 60 °C and measurement commenced. The core was first saturated with a 2% KCl solution with constant rate using a constatiometric pump. The chamber was then filled with fracturing fluids (with non-foamed fluid or a fluid with a 50% N_2 content) and a pressure of 6.89 MPa (1000 psi) was applied. After opening the valve at the bottom of the chamber, the measurement was initiated by measuring the value of filtration after 1, 4, 9, 16, 25, 36, 49 min. Taking into account data on the amount of filtrate as a function of time, the relationship between the amount of filtrate (cm^3) and the root of time ($min^{\frac{1}{2}}$) was plotted and leakoff coefficients were calculated: C_w and Spurt Loss (Figure 1, Table 1).

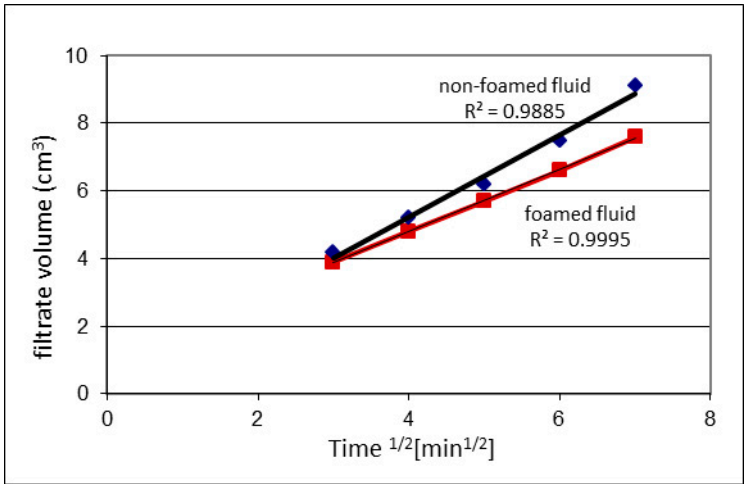

Figure 1. Filtrate volume as a function of square root of time with a trend line for fracturing fluids: non-foamed—blue line, foamed (50% of N_2)—red line.

Table 1. A comparison of leakoff coefficients C_w and Spurt Loss of Rotliegend cores for the tested fracturing fluids.

Non-Foamed Fluid		**Fluid 50% N_2**	
C_w ($m/min^{1/2}$)	Spurt (m^3/m^2)	C_w ($m/min^{1/2}$)	Spurt (m^3/m^2)
$5.373 \cdot 10^{-4}$	$3.473 \cdot 10^{-4}$	$4.057 \cdot 10^{-4}$	$9.904 \cdot 10^{-4}$

2.4. Simulation of Fracturing Treatment and Fracture Propagation

The obtained laboratory results: measurements of average cores permeability (0.14–0.16 mD), porosity (9–10%), parameters of filtration (Table 1) and viscosity coefficients (Tables 2 and 3) enabled the performance of computer simulations of hydraulic fracturing process in a vertical borehole using a 3D Fracpro computer simulator (Tables 4 and 5). For this purpose, a number of data were assumed for performing the simulations of hydraulic fracturing process, such as, e.g.: lithostratigraphy, Young's modulus, Poisson's ratio and stress gradient. Table 6 presents the data used for the construction of a geomechanical model, assuming the thickness of the productive horizon of approximately 25 m, with an insert of anhydrite.

Table 2. Rheological parameters of non-foamed fluids and fluids energized with N_2, foam quality of 50% at 23 °C.

Fluid Type	Time (min)	n' (-)	K' (Pa·s$^{n'}$)	Dynamic Viscosity at a Given Shear Rate (mPa·s)		
				40 s^{-1}	100 s^{-1}	170 s^{-1}
Non-foamed	9	0.6000	0.2154	49.2	34.1	27.6
	18	0.6006	0.2172	49.8	34.5	27.9
	27	0.5982	0.2224	50.5	34.9	28.2
50% N_2	9	0.4043	1.4727	163.6	94.8	69.1
	18	0.4038	1.4840	164.5	95.2	69.4
	27	0.3964	1.5414	166.2	95.6	69.4

Table 3. Rheological parameters of non-foamed fluids and energized with N_2 foam quality of 50% at 60 °C.

Fluid Type	Time (min)	n' (-)	K' (Pa·s$^{n'}$)	Dynamic Viscosity at a Given Shear Rate (mPa·s)		
				40 s^{-1}	100 s^{-1}	170 s^{-1}
Non-foamed	9	0.7674	0.0436	18.5	14.9	13.2
	18	0.7496	0.0475	18.9	15.0	13.1
	27	0.7620	0.0445	18.5	14.9	13.1
50% N_2	9	0.5801	0.4111	87.3	59.4	47.6
	18	0.5630	0.4618	92.1	61.7	48.9
	27	0.5652	0.4613	92.8	62.3	49.4

Table 4. Designed treatment schedule for non-foamed fluid.

Stage No.	Treatment Stage Type	Elapsed Time (min)	Fluid Type	Volume of Liquid without Proppant (m^3)	Proppant Concentration (g/L)	Proppant per Stage (kg)	Slurry Rate (m^3/min)	Proppant Type
-	Wellbore Fluid		2% KCL	11.26	-	-	-	
1	Main frac acid	1	15%HCl	5.00	0	0	4.0	-
2	Main frac flush	4	Non-foamed	12.00	0	0	4.0	-
3	Main frac pad	14	Non-foamed	40.00	0	0	4.0	-
4	Prop slug	19	Non-foamed	20.00	120	2400	4.0	100 mesh
5	Main frac pad	29	Non-foamed	40.00	0	0	4.0	-
6	Prop slug	34	Non-foamed	20.00	120	2400	4.0	100 mesh
7	Main frac pad	44	Non-foamed	40.00	0	0	4.0	-
8	Main frac slurry	49	Non-foamed	20.00	120	2400	4.0	30/50
9	Main frac pad	59	Non-foamed	40.00	0	0	4.0	-
10	Main frac slurry	65	Non-foamed	20.00	150	3000	4.0	30/50
11	Main frac pad	75	Non-foamed	40.00	0	0	4.0	-
12	Main frac slurry	80	Non-foamed	20.00	150	3000	4.0	30/50
13	Main frac pad	90	Non-foamed	40.00	0	0	4.0	-
14	Main frac slurry	95	Non-foamed	20.00	200	4000	4.0	30/50
15	Main frac pad	105	Non-foamed	40.00	0	0	4.0	-
16	Main frac slurry	111	Non-foamed	20.00	200	4000	4.0	30/50
17	Main frac pad	121	Non-foamed	40.00	0	0	4.0	-
18	Main frac slurry	126	Non-foamed	20.00	250	5000	4.0	30/50
19	Main frac pad	136	Non-foamed	40.00	0	0	4.0	-
20	Main frac slurry	142	Non-foamed	20.00	250	5000	4.0	30/50
21	Main frac pad	152	Non-foamed	40.00	0	0	4.0	-
22	Main frac slurry	157	Non-foamed	20.00	250	5000	4.0	30/50
23	Main frac pad	167	Non-foamed	40.00	0	0	4.0	-
24	Main frac slurry	173	Non-foamed	20.00	250	5000	4.0	30/50
25	Main frac pad	183	Non-foamed	40.00	0	0	4.0	-
26	Main frac slurry	188	Non-foamed	20.00	250	5000	4.0	30/50
27	Main frac flush	191	Non-foamed	11.00	0	0	4.0	-
28	Shut-in	221	SHUT-IN	0	0	0	0.0	-

Table 5. Design of the treatment schedule for foamed fluid.

Treatment Stage Type	Elapsed Time (min)	Fluid Type	Bottom N_2 Quality (%)	Bottom Clean Foam vol (m^3)	Bottom Proppant Concentration (g/L)	Proppant per Stage (kg)	Bottom Slurry Foam Rate (m^3/min)	Proppant Type
1	1	15% HCl	0	5.00	0	0	4.00	-
2	4	Non-foamed	0	12.00	0	0	4.00	-
3	6	Non-foamed	0	10.00	0	0	4.00	-
4	12	Non-foamed	0	20.00	120	2400	4.00	100 mesh
5	22	Non-foamed	0	40.00	0	0	4.00	-
6	27	Non-foamed	0	20.00	120	2400	4.00	100 mesh
7	37	Non-foamed	0	40.00	0	0	4.00	-
8	42	Non-foamed	0	20.00	120	2400	4.00	30/50
9	62	Non-foamed	0	40.00	0	0	2.00	-
10	73	N_2 50%	50.7	40.56	74	3000	3.95	30/50
11	93	N_2 50%	49.3	78.94	0	0	3.95	-
12	103	N_2 50%	51.6	41.28	121	5000	3.95	30/50
13	118	N_2 50%	49.3	59.20	0	0	3.95	-
14	135	N_2 50%	52.3	62.90	162	10,200	3.95	30/50
15	150	N_2 50%	49.3	59.20	0	0	3.95	-
16	167	N_2 50%	52.4	63.01	167	10,500	3.95	30/50
17	182	N_2 50%	49.3	59.20	0	0	3.95	-
18	199	N_2 50%	52.4	63.01	167	10,500	3.95	30/50
19	205	Non-foamed	0	11.00	0	0	2.00	-
20	220	SHUT-IN	0	0	0	0	0	-

Table 6. Reservoir parameters.

Layer Number	Top of Zone Measured depth (m)	Lithostratigraphy	Fracture Toughness (kPa·cm$^{1/2}$)	Young's Modulus (bar)	Poisson's Ratio	Stress Gradient (bar/m)
1	0	Overburden	21,976.9	4.14×10^5	0.250	0.190
2	2343	Salt	10,988.4	2.40×10^5	0.440	0.190
3	2463	Anhydrite	16,482.7	5.20×10^5	0.300	0.180
4	2479	Limestone	5494.2	1.00×10^5	0.300	0.180
5 *	2483	Rotliegend	10,988.4	2.00×10^5	0.245	0.170
6	2501	Anhydrite	16,482.7	5.20×10^5	0.300	0.180
7 *	2503	Rotliegend	10,988.4	2.00×10^5	0.245	0.170
8	2510	Anhydrite	16,482.7	5.20×10^5	0.300	0.180
9	2512	Sandstone	10,988.4	3.45×10^5	0.200	0.180
10	2660	Underlying rocks	21,976.9	4.14×10^5	0.250	0.190
11	3000	Underlying rocks	21,976.9	4.14×10^5	0.250	0.190

* productive horizon.

A very important aspect of analyzing treatment data using a simulator involves the selection of proper fracturing fluids parameters. Rheological parameters of the fluid directly affect the parameters of treatment, flow resistances and pressures in the well and fracture, slurry efficiency and the geometry of the generated fracture. The composition and rheological parameters of specific fluids are presented in Tables 2 and 3. During the simulation, other technological fluids were also used, e.g. 15% HCl. Table 7 presents a comparison between the parameters of simulated fracturing process performed by means of a non-foamed and foamed fluid.

Table 7. Basic data on simulated hydraulic fracturing operations.

	Non-Foamed Fluid	**Foamed Fluid**
	Quantity	
15% HCl	5.0 m^3	5.0 m^3
Linear gel 3.6 g/L	743.0 m^3	473.0 m^3
N_2	-	89,244.7 sm^3
Proppant 100 mesh	4800.0 kg	4800.0 kg
Proppant 30/50 mesh	41,399.9 kg	41,600.0 kg
Average pumping rate	4 m^3/min	4 m^3/min
Reservoir temperature in the perforation interval	60 °C	
Reservoir pressure in the perforation interval	250 bar	

When performing the simulation, the following were assumed: a comparable volume of treatments (the amount of liquid or foam and proppant) and a similar pumping plan and slurry rate.

3. Results and Discussion

3.1. The Results of Rheological Tests of Non-Foamed and Foamed Fluids

Rheological parameters are of key significance for fracturing fluids, since they largely decide about the geometry of the created fracture and transport properties for proppant materials during fracturing process. The rheological parameters (n' and K') of non-foamed and foamed fluids are presented on Figures 2 and 3 and in Tables 2 and 3, where n' is the dimensionless flow index and K' is the consistency factor.

Tables 2 and 3 present test results for foamed fracturing fluids with 50% foam quality and non-foamed fluids. A drop in viscosity along with an increase in temperature is particularly visible for non-foamed fluids (Tables 2 and 3). A non-foamed fluid with a quality of 50%, whose viscosity in the ambient temperature was approximately 35 cP, with a shear rate of 100 s^{-1}, upon heating up to 60 °C dropped to a viscosity of 15 cP. For foamed solutions of polymer W-1, a considerably higher viscosity is observed compared to non-foamed fluids. The viscosity of foamed fluids at a temperature of 23 °C with a shear rate of 100 s^{-1} is approximately 3-fold higher, and about 4-fold higher at a temperature of 60 °C compared to non-foamed fluids.

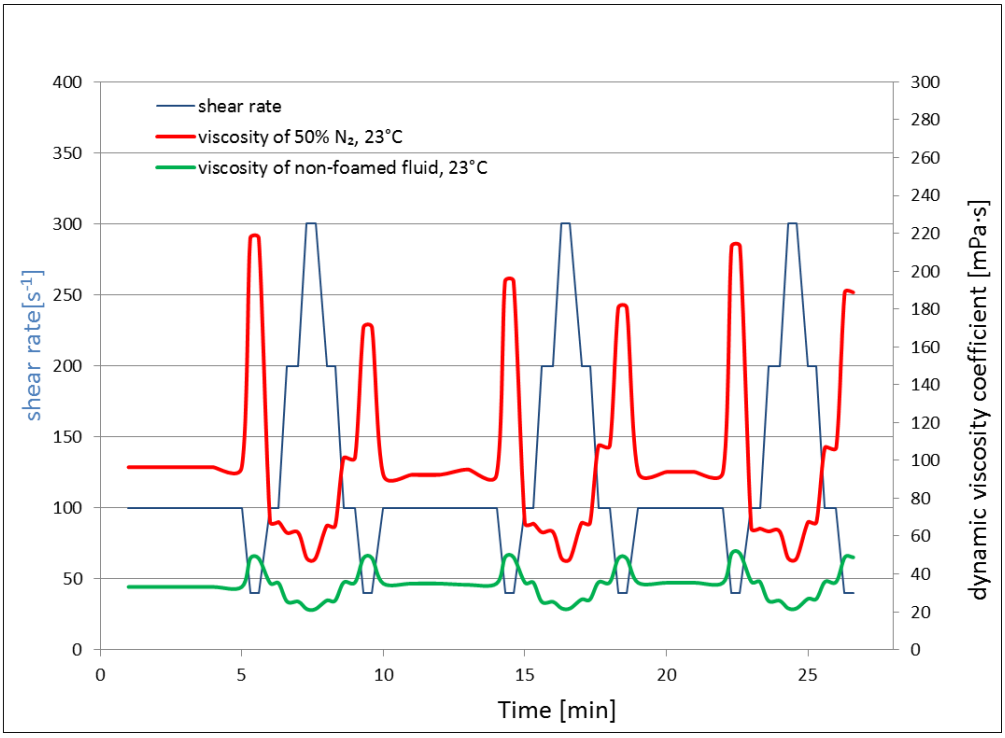

Figure 2. Viscosity of non-foamed and 50% N_2 foamed fluid with addition of 3.6 g/L natural polymer at 23 °C.

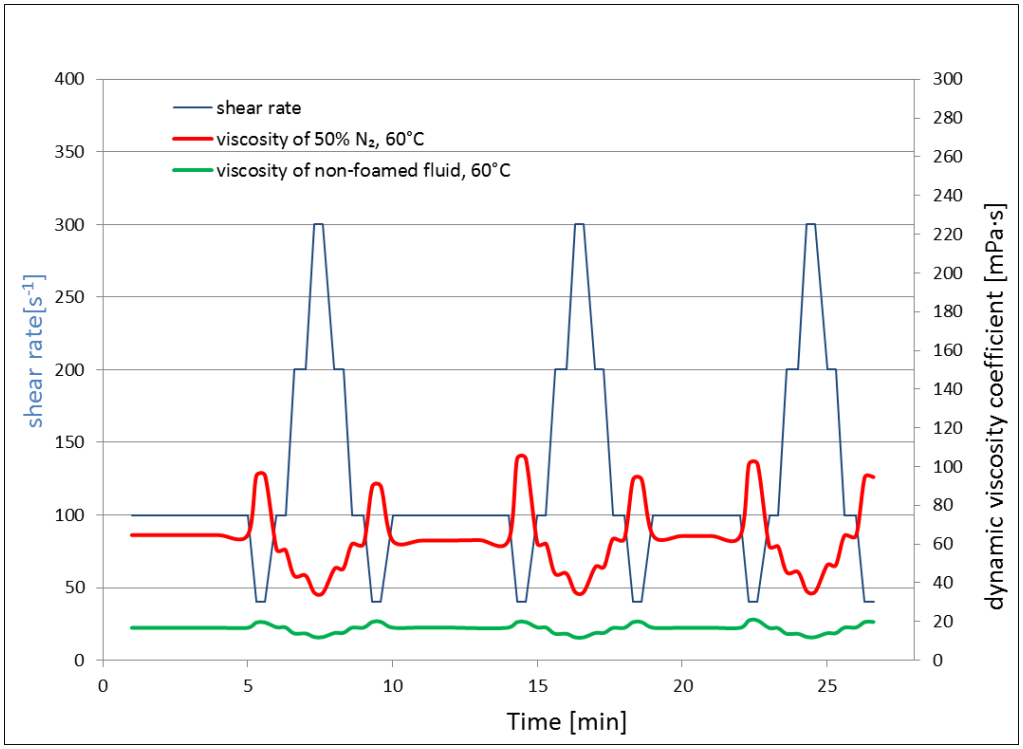

Figure 3. Viscosity of non-foamed and N_2 foamed fluid with addition of natural polymer in an amount of 3.6 g/L at 60 °C.

3.2. Filtration Test Results

The filtration test was performed for Rotliegend cores using a non-foamed fracturing fluids and a fluid foamed by 50% of N_2 (Figure 1, Table 1).

The C_w coefficient is directly proportional to the speed of filtration through the generated filter cake. On the other hand, the Spurt value approximates the volume of fluid which was filtered out during the generation of the filter cake. Leakoff coefficients calculated based on the measurements (Table 1) were used for simulation assumptions presented in the following part of the paper. The leakoff coefficient was lower for a foamed fluid than for a single-phase fluid. This may have been caused by the penetration of gas bubbles into rock pores, which impedes the escape of liquid from a fracture. It should be mentioned that observations were performed based on relatively short filtration tests according to the guidelines of quality standard API RP39. In this case, the generation of a filtration cake is a key phenomenon at the initial stage of flow of a fluid through the core. This process is strictly associated with rock permeability, since at the beginning of the fracturing process filtration depends on the permeability of the formation. At the next stage, in the case of gelled single-phase fluids it is controlled by the filter cake formation on the walls of the fracture, whose permeability is lower than the permeability of the reservoir rock. This causes an increase in the slurry efficiency, because its smaller volume penetrates from the fracture to reservoir during the treatment. This also implies a lower invasion of liquid into the zone surrounding a hydraulically generated fracture. This enables easier clean-up of the reservoir formation after the fracturing process.

It has been observed that the foam generated based on the gelled fluid also causes the creation of filter cake on the fracture walls, but its thickness is smaller than in the case of single-phase fluids; nonetheless, filtration is often lower for foam, due to the penetration of gas into the rock formation, which decreases its phase permeability. Due to this, for foams generated using linear gel, it is possible to minimize damage to the formation during the fracturing process.

3.3. 3D Simulation Results

Figures 4 and 5 present a simulation of the fracturing process with non-foamed and nitrogen-foamed fluids, along with the most important parameters of the process, such as: net pressure, bottom hole pressure, surface pressure, concentration of proppant, slurry rate and efficiency of the fracturing fluids. The pumping schedules differ from each other, which was forced by initial assumptions of using similar volumes of fluid and proppant in both cases of the simulated treatment. Originally, the maximum pressure at the surface (at pumping units), in both cases of using foamed and non-foamed fluid, amounts to 518 bar, and it equals the opening pressure of the fracture. During the treatment, it is definitely lower in the case of non-foamed fluid and amounts to approximately 330–350 bar. In the case of foamed fluid, at the beginning of the procedure it amounts to approximately 350 bar, upon which it increases to approximately 500 bar in the second part of the process. During the use of a non-foamed fluid, the slurry rate is pumped at 4 m^3/min. In the case of foamed fluid, a non-foamed linear polymer is injected until stage 9 of pumping (Table 4), while nitrogen is added from stage 10 to 18 in an amount of 50% relative to the pumped linear gel. Figure 4 presents the pumping rate of linear gel which amounts to approximately 2 m^3/min, and N_2 is introduced at the same rate. Net pressure—one of the most important parameters during the fracturing treatment—as the difference between the bottom dynamic pressure during treatment and the fracture closure pressure [38–40], behaves similarly in both simulated cases. Maximum value is reached at the end of fracturing treatments and amounts to 76.1 bar for non-foamed fluid and 83.9 bar for foamed fluid, respectively. The efficiency of non-foamed fluid (Figure 4) increases slowly during the performed fracturing, due to a gradual stabilization of the filter cake generated on the fracture surface. Close to the end of fracturing, this value amounts to 0.49. The efficiency of foamed fluid (Figure 5) is constant until stage 8 of pumping; then it decreases in the pumping stage 9, which is caused by a decrease in the fluid rate (therefore, there is a decrease in the fracture). When pumping a foamed fluid, its efficiency improves considerably, and reaches a value of 0.50 at the end of treatment.

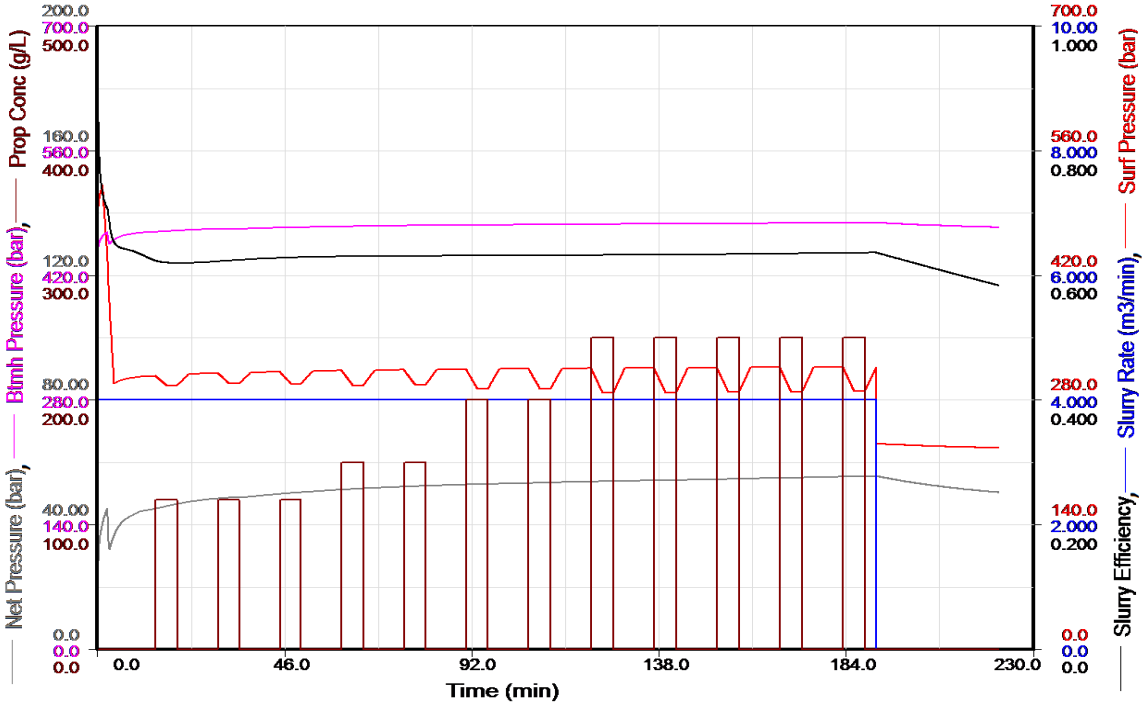

Figure 4. Treatment data for non-foamed fluid.

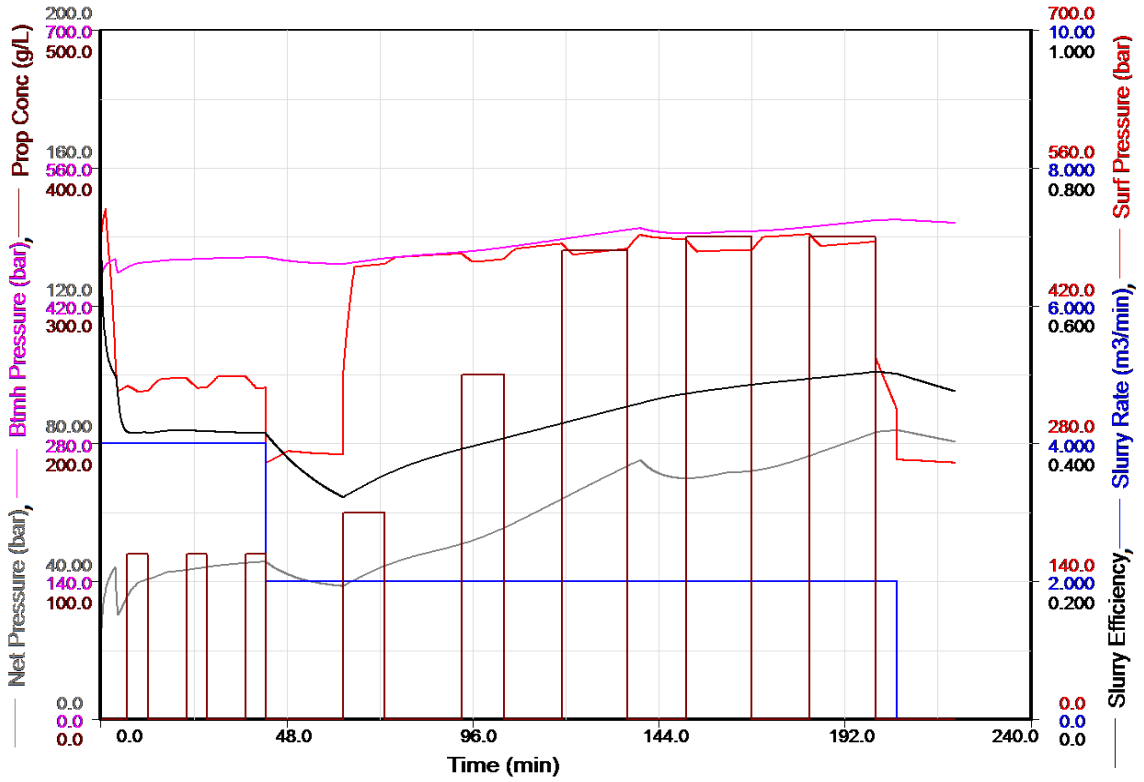

Figure 5. Treatment data for foamed fluid.

Figures 6 and 7 present the characteristics of fractures generated in the simulation, and a summary as well as list of values describing the fractures are presented in Table 8. When using non-foamed fluid, the fracture is slightly longer and higher compared to foamed fluid, while its width is smaller. When fracturing with the foam, the proppant placement in the Rotliegend productive horizon (Figure 6) is much more preferable in terms of the treatment performance, while high concentration of

the proppant in the case of using a non-foamed fluid is obtained only in the top part of the Rotliegend productive horizon (Figure 7). Foamed fluid increases the viscosity of fracturing fluid and higher fluid viscosity increases fracture width and eases the improved proppant placement and transport of proppant into the formation. Fracture geometry details and other important treatment data are presented in Table 8 as a stimulation treatment comparison.

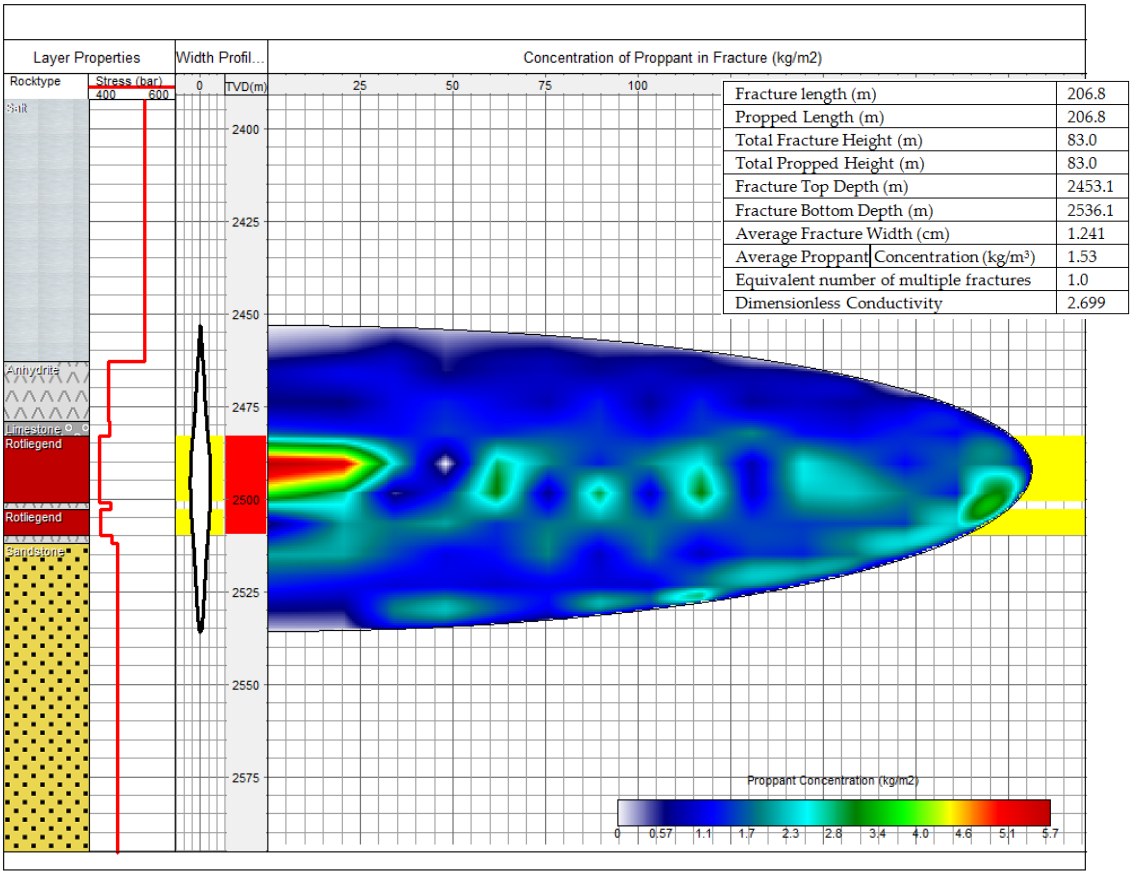

Figure 6. Fracture profile and layers for non-foamed fluid.

The final result of the simulation is a technical plan which describes in detail how the fracturing treatment is to be performed. One of the essential parts of this plan is the pumping schedule, which includes the information on: what, when, in what amount, with what capacity and with what pressure will be pumped into the fractured reservoir (Tables 7 and 8; Figures 4 and 5). However, before a technical plan is developed and the hydraulic fracturing treatment is performed in the borehole, it is necessary to carry out tests intended to confirm or correct key reservoir data [41]. Nonetheless, due to the complex nature of hydraulic fractures and very low permeability of tight reservoirs, to predict the performance of gas production of such complicated reservoirs is very difficult. The best way to improve these methods' accuracy is combining them by the numerical simulations to production, because there are areas where commercial simulators reaches unrealistic estimates unacceptable for shale/tight gas reservoirs [42]. Jia [43] highlights the importance of production simulations which should take into account the complex-flow behaviors in both fractures and the matrix. After performing comprehensive sensitivity analysis, it was recognized that natural-fracture spacing was the most prominent factor affecting shale gas reservoir performance. Simulation results of tight gas formation by foam compared to simulating conventional treatment, in this paper, could guide to more accurate reservoir modeling regarding tight gas production.

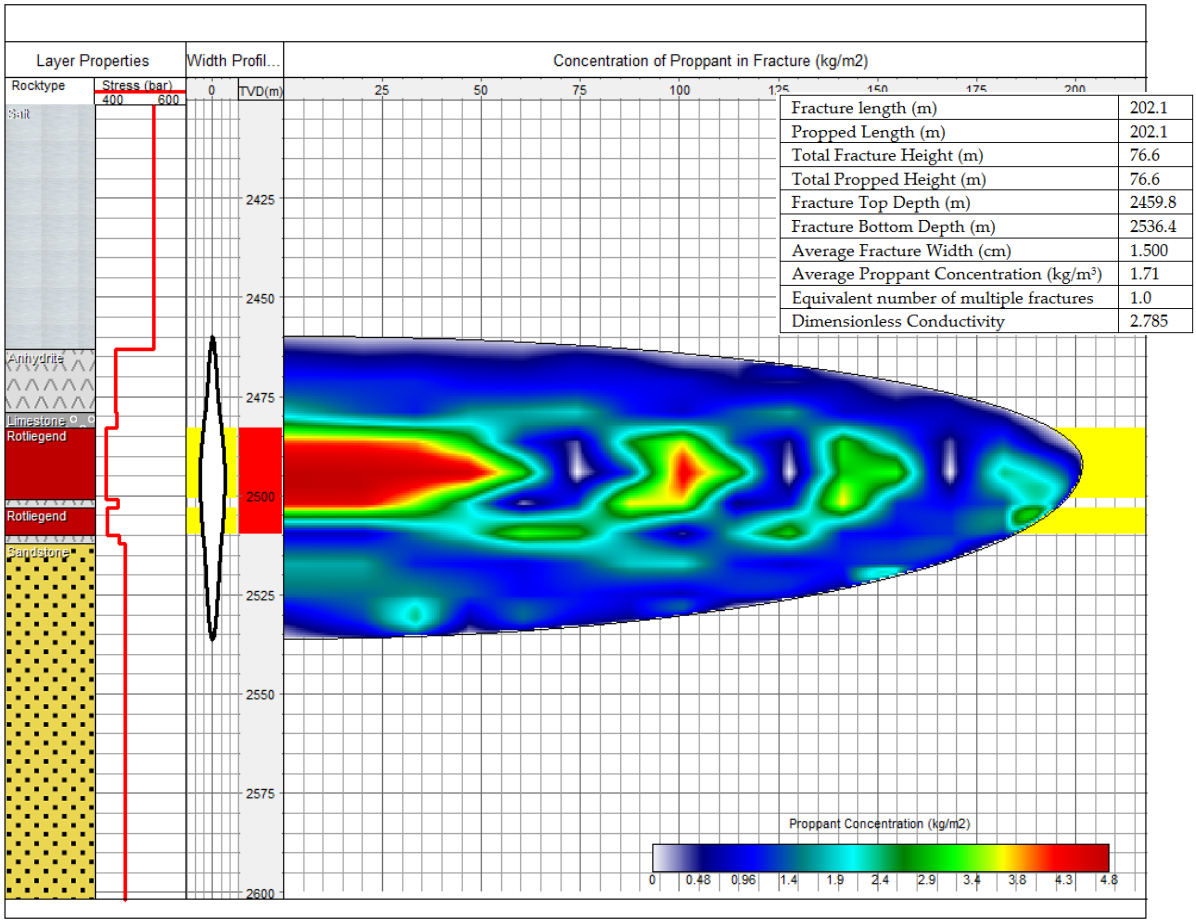

Figure 7. Fracture profile and layers for foamed fluid.

Table 8. Stimulation treatment comparison.

Parameters	Non-Foamed Fluid	Fluid 50% N_2
Fracture Length (m)	206.8	202.1
Propped Length (m)	206.8	202.1
Total Fracture Height (m)	83.0	76.6
Total Propped Height (m)	83.0	76.6
Fracture Top Depth (m)	2453.1	2459.8
Fracture Bottom Depth (m)	2536.1	2536.4
Average Fracture Width (cm)	1.2	1.5
Average Proppant Concentration (kg/m^2)	1.5	1.7
Dimensionless Conductivity	2.699	2.785
Total Clean Fluid Pumped (without proppant) (m^3)	750.8	750.1
Total Slurry Pumped (with proppant) (m^3)	766.2	765.5
Design proppant pumped (kg)	46,200	46,400

4. Conclusions

The following conclusions were drawn based on the experimental results and the findings of the study:

1. For the simulated treatments with foamed and non-foamed fluid, with the same amounts of proppant and base fluid (Tables 7 and 8) the resulting values of average surface concentration of the proppant inside a fracture and its conductivity were similar (1.5 and 1.7 kg/m^2 respectively).
2. Based on laboratory tests and simulations, it can be concluded that foamed fluids exhibit good rheological parameters and capability of opening a fracture (Figures 5 and 6; Table 8) and

proppant-carrying capacity, which is crucial during fracturing treatment. In general: similar geometries of the fracture and proppant concentrations are obtained for the non-foamed as well as for 50% quality nitrogen foamed fluids. At the same time, when using a fluid with a gas additive, the water content in fracturing fluid is reduced, up to 50%, which means the minimization of the negative results of the clay minerals swelling.

3. When using non-foamed fluid, the fracture is slightly longer (4.7 m) and higher (6.4 m) compared to foamed fluid, while its width is smaller (0.3 cm less). When fracturing with the foam, the placement of the proppant in the productive horizon is much more beneficial in terms of the fracturing treatment performance. High concentration of the proppant, in the case of using a non-foamed fluid, is obtained only in the top part of the Rotliegend productive horizon, causing an irregular proppant distribution in the fracture (Figures 6 and 7).
4. The analysis of laboratory data (Table 8), and the performed simulations indicated that fracturing fluids foamed by nitrogen are a good alternative to conventional fluids (non-foamed), especially for the low-pressure reservoirs and with high sensitivity to contact with water.

Funding: Part of the research leading to these results was prepared on the basis of statutory study financed by Ministry of Science and Higher Education—archival no.: 0040/KS/19, order no.: DK-4100-40/19.

Conflicts of Interest: The author declares no conflict of interest.

References

1. Sorrell, S.; Speirs, J.; Bentley, R.; Brandt, A.; Miller, R. Global oil depletion: A review of the evidence. *Energy Policy* **2010**, *38*, 5290–5295. [CrossRef]
2. Bentley, R.W. Global oil & gas depletion: An overview. *Energy Policy* **2002**, *30*, 189–205.
3. Wu, Y.; Li, X. Numerical Simulation of the Propagation of Hydraulic and Natural Fracture Using Dijkstra's Algorithm. *Energies* **2016**, *9*, 519. [CrossRef]
4. Shonkoff, S.B.; Hays, J.; Finkel, M.L. Environmental Public Health Dimensions of Shale and Tight Gas Development. *Environ. Health Perspect.* **2014**, *122*, 787–795. [CrossRef] [PubMed]
5. Al-Muntasheri, G. A Critical Review of Hydraulic Fracturing Fluids for Moderate-to-Ultralow-Permeability Formations over the Last Decade, SPE-169552-PA. *SPE Prod. Oper.* **2014**, *29*. [CrossRef]
6. Rozell, D.J.; Reaven, S.J. Water pollution risk associated with natural gas extraction from the Marcellus Shale. *Risk Anal.* **2012**, *32*, 1382–1393. [CrossRef] [PubMed]
7. Wilk, K.; Kasza, P.; Labus, K. Analysis of the applicability of foamed fracturing fluids. *Nafta Gaz* **2015**, *6*, 425–433.
8. Hutchins, R.D.; Miller, M.J. A Circulating Foam Loop for Evaluating Foam at Conditions of Use. *SPE Prod. Facil.* **2005**, *20*. [CrossRef]
9. Gidley, J.L.; Holditch, S.A.; Nierode, D.E.; Veatch, R.W. *Recent Advances In Hydraulic Fracturing*; SPE Monograph Series; Society of Petroleum Engineers of AIME: Richardson, TX, USA, 1990; Volume 12, p. 464.
10. Wanniarachchi, W.A.M.; Ranjith, P.G.; Perera, M.S.A. Shale gas fracturing using foam-based fracturing fluid: A review. *Environ. Earth Sci.* **2017**, *76*, 1–15. [CrossRef]
11. Wanniarachchi, W.A.M.; Ranjith, P.G.; Perera, M.S.A.; Lashin, A.; Al Arifi, N.; Li, J.C. Current opinions on foam-based hydro-fracturing in deep geological reservoirs. *Geomech. Geophys. Geo-Energy Geo-Resour.* **2015**, *1*, 121–134. [CrossRef]
12. Small, X.T. Water Use and Recycling in Hydraulic Fracturing: Creating a Regulatory Pilot for Smarter Water Use in the West. *Nat. Resour. J.* **2015**, *55*, 409–440.
13. Freeman, B. Engineers improve recycling system used in fracking to save water and energy. *Membr. Technol.* **2013**, *2013*, 7. [CrossRef]
14. McAndrew, J.J.; Fan, R.; Sharma, M.; Ribeiro, L. Extending the application of foam hydraulic fracturing fluids. In Proceedings of the SPE/AAPG/SEG Unconventional Resources Technology Conference, Denver, CO, USA, 25–27 August 2014. [CrossRef]
15. Labus, K. Potential environmental problems connected with the exploitation of unconventional natural gas deposits. *Przegląd Górniczy* **2011**, *67*, 12–16.

16. Tulissi, M.G.; May, R.E. A Comparison of Results of Three Different CO_2 Energized Frac Fluids: A Case History. SPE-75681-MS. In Proceedings of the SPE Gas Technology Symposium, Calgary, AB, Canada, 30 April–2 May 2002.
17. Faroughiab, S.A.; Pruvota, A.J.-C.J.; McAndrewa, J. The rheological behavior of energized fluids and foams with application to hydraulic fracturing: Review. *J. Pet. Sci. Eng.* **2018**, *163*, 243–263. [CrossRef]
18. Turek, M.; Labus, K.; Dydo, P.; Mitko, K.; Laskowska, E.; Jakóbik-Kolon, A. A concept of hydraulic fracturing flowback treatment using electrodialysis reversal. *Desalin. Water Treat.* **2017**, *64*, 228–232. [CrossRef]
19. Torabzadeh, J.; Langnes, G.L.; Robertson, J.O., Jr.; Yen, T.F.; Donaldson, E.C.; Chilingarian, G.V.; Yen, T.F. *Enhanced Oil Recovery, II: Processes and Operations*; Elsevier Science Publishers B. V.: Amsterdam, The Netherlands, 1989; pp. 91–106.
20. Harris, P.C. High-Quality Foam Fracturing Fluids. In Proceedings of the SPE Gas Technology Symposium, Calgary, AB, Canada, 28 April–1 May 1996. [CrossRef]
21. Blauer, R.E.; Kohlhaas, C.A. Formation Fracturing with Foam. SPE-5003-MS. In Proceedings of the Fall Meeting of the Society of Petroleum Engineers of AIME, Houston, TX, USA, 6–9 October 1974. [CrossRef]
22. Cawiezel, K.E.; Niles, T.D. Rheological Properties of Foam Fracturing Fluids Under Downhole Conditions. SPE-16191-MS. In Proceedings of the SPE Production Operations Symposium, Oklahoma, OK, USA, 8–10 March 1987.
23. Temizel, C.; Energy, A.; Betancourt, D.; Aktas, S.; Susuz, O.; Zhu, Y.; Suhag, A.; Ranjith, R.; Wang, A. Optimization of Hydraulic Fractures in Tight-Oil Reservoirs Using Different Numerical Fracture Models. In Proceedings of the SPE Asia Pacific Hydraulic Fracturing Conference, Beijing, China, 24–26 August 2016; SPE-181824-MS. pp. 1–58.
24. Acharya, R. Hydraulic-Fracture-Treatment Design Simulation. *J. Pet. Technol.* **1988**, *40*, 139–142. [CrossRef]
25. Shahkarami, A.; Wang, G.; Belyadi, H. Horizontal Well Spacing and Hydraulic Fracturing Design Optimization: A Case Study on Utica-Point Pleasant Shale Play. In Proceedings of the Unconventional Resources Technology Conference, San Antonio, TX, USA, 1–3 August 2016; pp. 1–12.
26. Shah, K.; Shelley, R.F.; Gusain, D.; Lehman, L.V.; Mohammadnejad, A.; Conway, M.T. Development of the Brittle Shale Fracture Network Model. SPE-163829-MS. In Proceedings of the SPE Hydraulic Fracturing Technology Conference, The Woodlands, TX, USA, 4–6 February 2013.
27. Zhang, S.-C.; Lei, X.; Zhou, Y.-S.; Xu, G.-Q. Numerical simulation of hydraulic fracture propagation in tight oil reservoirs by volumetric fracturing. *Pet. Sci.* **2015**, *12*, 674. [CrossRef]
28. Zhou, L.; Guo, J. 3D Modeling of Hydraulic Fracturing in Tight Gas Reservoirs by Using of FLAC3D and Validation through Comparison with FracPro. *Adv. Mater. Res.* **2012**, *524–527*, 1293–1299. [CrossRef]
29. McAndrew, J.; Fan, R.; Barba, R. Energized and foam fracturing fluids for liquids-rich organic shale reservoirs. In Proceedings of the AAPG 2014 Annual Convention & Exhibition, Houston, TX, USA, 6–9 April 2014.
30. Fei, Y.; Gonzalez Perdomo, M.E.; Pokalai, K.; Haghighi, M. 3D Simulation of Hydraulic Fracturing by Foam Based Fluids Using a Fracture Propagation Model Coupled with Geomechanics in an Unconventional Reservoir the Cooper Basin, South Australia. In Proceedings of the International Conference on Geomechanics, Geo-energy and Geo-resources, Chengdu, China, 21–24 September 2018.
31. Gu, M.; Mohanty, K. Rheology of polymer-free foam fracturing fluids. *J. Pet. Sci. Eng.* **2015**, *134*, 87–96. [CrossRef]
32. Gu, M. Shale fracturing enhancement by using polymer-free foams and ultra-light weight proppants. Ph.D. Thesis, The University of Texas at Austin, Austin, TX, USA, 2013.
33. Wright, C.A.; Weijers, L.; Davis, E.J.; Mayerhofer, M. Understanding Hydraulic Fracture Growth: Tricky but Not Hopeless. SPE 56724. In Proceedings of the SPE Annual Technical Conference and Exhibition, Houston, TX, USA, 3–6 October 1999. [CrossRef]
34. Wilk, K.; Kasza, P.; Czupski, M. Dodatki do spienionych płynów szczelinujących. *Przemysł Chem.* **2018**, *92*, 1000–1005. [CrossRef]
35. Wilk, K.; Kasza, P.; Czupski, M. Dobór dodatków do energetyzowanych płynów szczelinujących. *Nafta Gaz* **2016**, *12*, 1092–1100. [CrossRef]
36. Wilk, K.; Kasza, P.; Labus, K. Impact of nitrogen foamed stimulation fluids stabilized by nanoadditives on reservoir rocks of hydrocarbon deposits. *Nanomaterials* **2019**, *9*, 766. [CrossRef]
37. *Recommended Practice for Standard Procedure for evaluation of Hydraulic Fracturing Fluids*; American Petroleum Institute: Washington, DC, USA, 1983.

38. Kasza, P. Zabiegi hydraulicznego szczelinowania w formacjach łupkowych. *Nafta Gaz* **2011**, *12*, 874–883.
39. Belyadi, H.; Fathi, E.; Belyadi, F. Fracture Pressure Analysis and Perforation Design. In *Hydraulic Fracturing in Unconventional Reservoirs Theories, Operations, and Economic Analysis*; Gulf Professional Publishing: Houston, TX, USA, 2017; pp. 121–141. [CrossRef]
40. Guo, B.; Liu, X.; Tan, X. Chapter 14—Hydraulic Fracturing. In *Petroleum Production Engineering*, 2nd ed.; Gulf Professional Publishing: Houston, TX, USA, 2017; pp. 389–501. ISBN 9780128096123.
41. Kasza, P. Zabiegi hydraulicznego szczelinowania złóż niekonwencjonalnych i metody ich analizy. *Pr. Nauk. Inst. Naft. i Gazu* **2019**, *226*, 1–147.
42. Andrade, J.; Civan, F.; Devegowda, D.; Sigal, R. Accurate Simulation of Shale Gas Reservoirs. SPE-135564-MS. In Proceedings of the SPE Annual Technical Conference and Exhibition, Florence, Italy, 19–22 September 2010. [CrossRef]
43. Jia, B.; Tsau, J.-S.; Barati, R. *Investigation of Shale-Gas-Production Behavior: Evaluation of the Effects of Multiple Physics on the Matrix*; SPE-197069-PA; Society of Petroleum Engineers: Houston, TX, USA, 2019. [CrossRef]